ACS Energy LETTERS

http://pubs.acs.org/journal/aelccp

REVIEW

Electrolyte Engineering for Long-Life Li-SPAN Batteries

Qiushi Miao,[+] Nicholas Solan,[+] Gayea Hyun, John Holoubek,* and Ping Liu*

Cite This: *ACS Energy Lett.* 2023, 8, 4818−4830

Read Online

ACCESS | Metrics & More | Article Recommendations | Supporting Information

ABSTRACT: Sulfurized polyacrylonitrile, or SPAN, has been studied as an alternative to elemental sulfur as a cathode in lithium−sulfur batteries. Unlike elemental S, the material features a solid-phase conversion reaction during charge and discharge, which shows promise in providing long cycle life under lean electrolyte conditions. However, this altered mechanism also imposes a unique set of electrolyte design requirements. In this Review, we outline the key advancements in electrolyte engineering and discuss the design principles of these electrolytes with a focus on the solvation structures and their ability to control the interphasial chemistry on both the Li and the SPAN surfaces. We then argue for the need to develop electrolytes with improved transport properties while preserving their high stabilities in order to realize Li-SPAN batteries with practical energy densities.

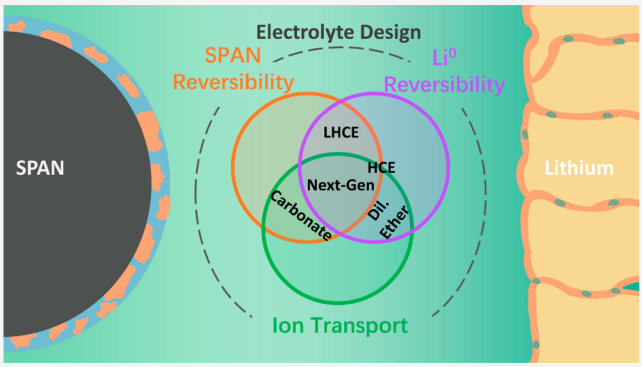

Lithium−sulfur (Li-S) batteries are potentially low-cost, high-energy-density options for powering next-generation mobility and stationary systems. Sulfur has a high specific capacity of 1676 mAh g^{-1} through a 2-electron reduction process and is earth-abundant, with no supply chain concerns. However, challenges are well documented for Li-S batteries.[1−4] The insulating nature of elemental S necessitates a solution-mediated process, where the discharge intermediate products, lithium polysulfides (PSs), dissolve in the electrolyte during operation (Figure 1a). While this process enhances reaction kinetics, it also introduces the well-known "shuttle" phenomenon, where soluble PSs reach the lithium anode, essentially creating an internal short and contributing to the (electro)chemical degradation of both electrodes over time. Although nanoporous carbon has been widely applied as a S host to enhance electronic conductivity, to provide a framework structure to manage volume change, and to restrict the diffusion of PSs,[4] this approach does not fundamentally alter the reaction pathway. As a result, the nature of liquid-phase redox fundamentally links the performance of the battery with the applied electrolyte volume, limiting practical energy densities of Li-S batteries due to the high electrolyte-to-capacity ratio, or E/C (Figure 1c).[5] This is reflected in an inverse relationship between cycle life and energy density, which has plagued the advent of Li-S cells at scale.[5]

Fortunately, altering the chemical environment of electrochemically active S provides a means to circumvent the negative externalities of liquid-phase redox. Sulfurized polyacrylonitrile (SPAN) is a prototypical sulfur-containing polymer material and holds great promise to serve as sulfur-based cathode for next-generation Li metal batteries. SPAN is readily synthesized by heating polyacrylonitrile (PAN) with elemental S, during which the PAN units cyclize to form a network of conjugated pyridine rings, on which S is stabilized via covalent bonding. During cycling, the -S_x- ($x < 4$) species existing in SPAN materials undergo a solid−solid conversion reaction without the involvement of soluble PSs.[6] As demonstrated in their voltage profiles, Li-SPAN batteries display a gradual slope during charge and discharge, indicative of a solid−solid conversion process (Figure 1b). This contrasts with the typical dual-voltage plateau process in Li-S batteries characteristic of two-phase conversions between polysulfide species (Figure 1a). This solid conversion mechanism is partially enabled by the much higher electronic conductivity of SPAN of 10^{-7} to 10^{-5} S cm^{-1} due to the conjugated carbon network.[7] This contrasts with 10^{-30} S cm^{-1} for S,[8] and 10^{-9} S cm^{-1} for Li_2S.[9] The lack of the involvement of PS dissolution leads to reported high cycling stability and high sulfur utilization. Typically, SPAN shows a high sulfur utilization of

Received: August 17, 2023
Accepted: October 3, 2023
Published: October 23, 2023

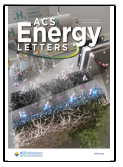

https://doi.org/10.1021/acsenergylett.3c01711
ACS Energy Lett. 2023, 8, 4818−4830

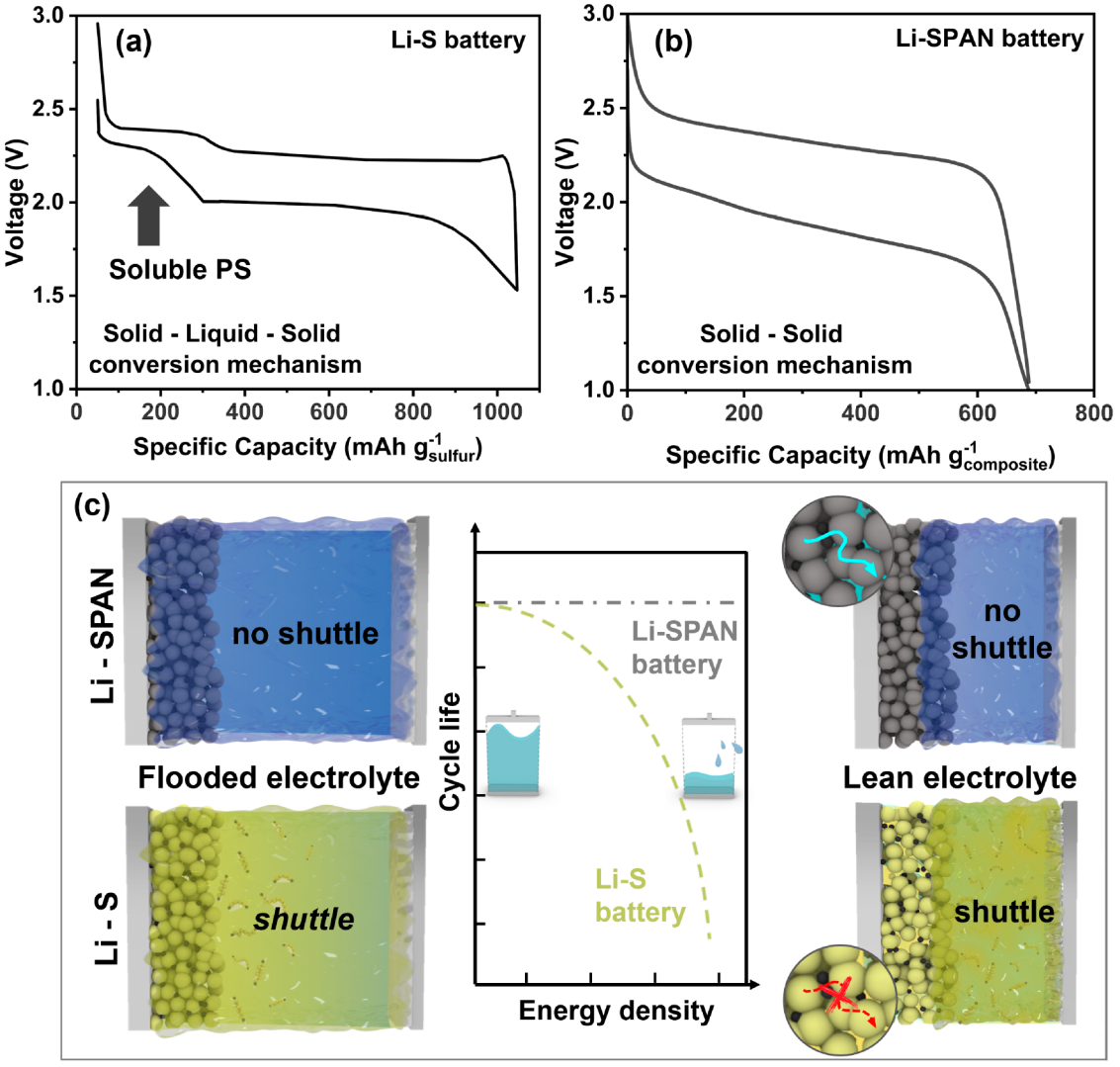

Figure 1. Comparison between Li-S and Li-SPAN regarding their operating mechanism and sensitivity to electrolyte amount. Schematic diagrams for charge and discharge voltage profiles for (a) Li-S batteries with a solid−liquid−solid conversion mechanism and (b) Li-SPAN batteries with a solid−solid conversion mechanism. (c) Schematic diagram showing the impact of electrolyte amount on electrochemical performance of Li-S batteries and Li-SPAN batteries.

above 90%,[10−13] compared to typical sulfur utilization of below 70% in elemental S cathodes with similar loadings.[14] Cell performance is thus much less sensitive to the E/C ratio (Figure 1c). The optimum electrolyte loading is dictated by the cyclability of the Li metal anode and the porosity of the cathode, rather than by the need to dissolve polysulfides. A Li-SPAN pouch cell reported in 2021 used a 12 mg cm^{-2} SPAN cathode, with an E/C of 1.24 g Ah^{-1} (assuming the density of the electrolyte is 1.87 g mL^{-1}), and showed a capacity retention of 95% after 150 cycles,[15] while a Li-S pouch cell with a sulfur loading of 6 mg cm^{-2} and E/C ratio of 3.3 g Ah^{-1} only cycled for 35 cycles, with a capacity retention of 31%.[5]

Though practical Li-SPAN batteries are within closer reach than Li-S, their advent depends on the development of compatible electrolytes. These electrolytes are tasked with maintaining the solid−solid conversion mechanism enjoyed by the SPAN cathode, as well as enabling high-efficiency cycling of the Li anode. SPAN cathodes, lacking pre-lithiation, necessitate their pairing with Li-metal anodes. Owing to the inherently low voltage of sulfur-based cathodes, the practical requirement exposes lithium to a heightened risk of experiencing an elevated current density to operate at a reasonable C-rate compared with typical oxide-based cathode materials. While a variety of approaches, e.g., 3D hosts,[16,17] surface coatings,[18,19] and substrate engineering,[20] are being explored to improve the reversibility of the Li anode, electrolyte development remains a focus for the community.

The development of electrolyte for the Li-SPAN batteries has been the subject of several previous reviews.[21−23] These reviews have examined the effect of electrolyte components (solvents, salts, and additives) on cell performance and their interactions with both the lithium anode and the SPAN cathode. In this Review, we outline the significant conceptual advances of electrolyte development for the Li-SPAN system, with a special focus on the role of electrolytes in forming stable interphasial layers on both the anode and the cathode. This conceptual framework enables us to examine the historical trajectory of Li-SPAN battery electrolyte development as well as to offer perspectives for future research directions that will enable the Li-SPAN chemistry to deliver on its full promise of low cost, high energy density, and long cycle life.

https://doi.org/10.1021/acsenergylett.3c01711
ACS Energy Lett. 2023, 8, 4818−4830

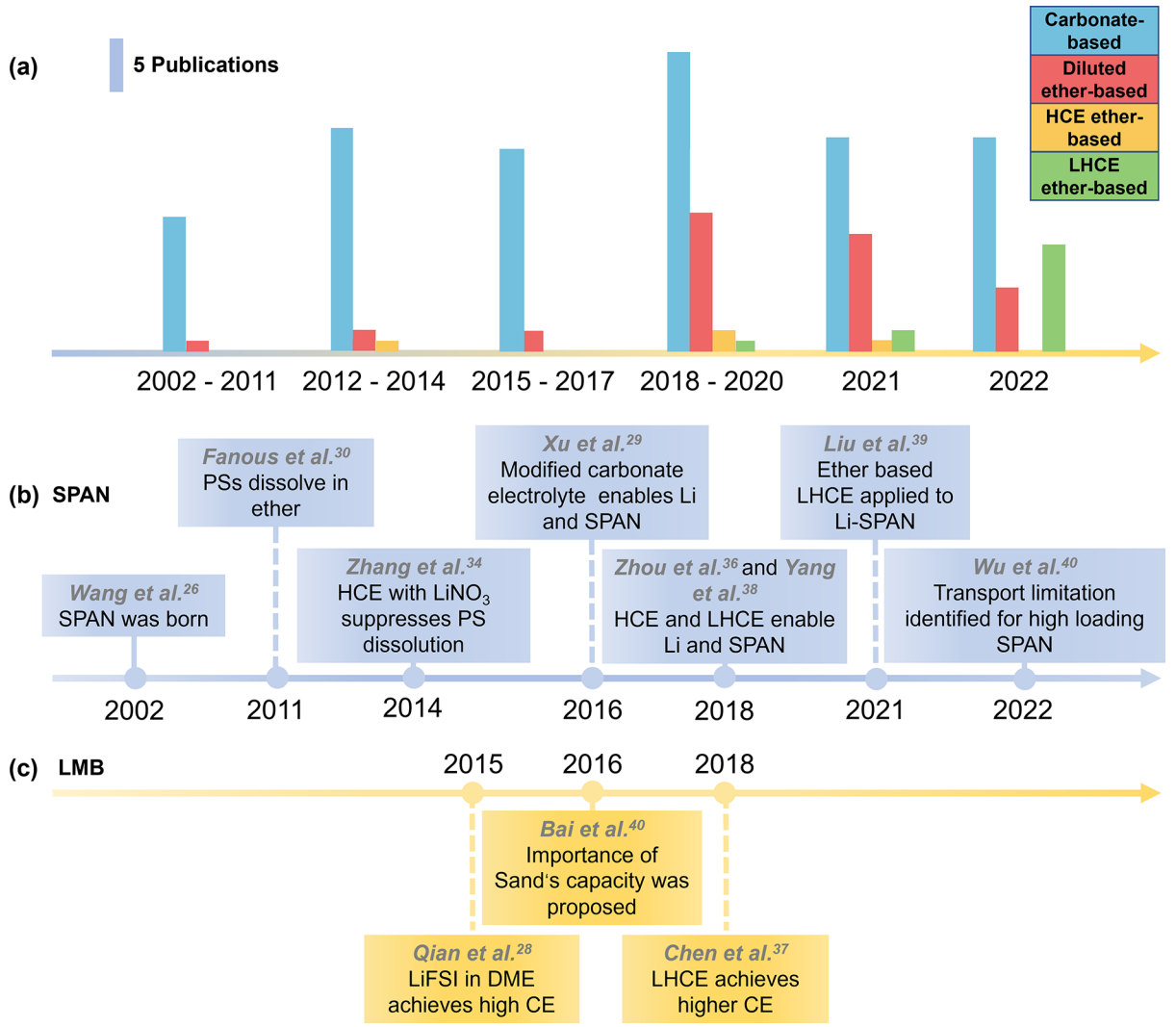

Figure 2. Timeline for electrolyte development for Li-SPAN batteries. (a) Number of publications for four classes of electrolytes. (b) Representative electrolytes introduced over time to address performance issues of Li-SPAN batteries. (c) Electrolytes introduced to improve lithium metal cycling stability, which often inspired similar approaches to Li-SPAN.

Li-SPAN ELECTROLYTE TIMELINE

Figure 2 summarizes the history of electrolyte development for Li-SPAN batteries. We categorize the electrolytes into four families: carbonate (blue), diluted ether (red), high-concentration electrolyte (HCE) based on ether (yellow), and localized high-concentration electrolyte (LHCE) based on ether (green). HCE refers to electrolytes containing high concentrations of salts such that the solvation structure of Li^+ ions deviates from that in dilute electrolytes.[24] LHCEs are formulated from HCEs by adding a non-solvating, often fluorinated diluent, which reduces the viscosity, improves wetting, and may increase conductivity.[25] Figure 2a shows the number of papers published for the different categories over time. A comprehensive compilation of the references is provided in Table S1. Carbonate-based electrolytes have been the overwhelming favorite. However, since 2020, there is a clear increase in the application of ether-based LHCEs. As discussed below, this transition has been driven by the need for electrolytes that enable stable cycling for both the SPAN cathode and the Li anode. Figure 2b outlines several milestones in the development of electrolytes for Li-SPAN batteries, while Figure 2c shows three developments in Li anode research that have significantly impacted the progress of the Li-SPAN system.

> The transition from carbonate-based electrolytes to ether-based localized high-concentration electrolytes has been driven by the need for electrolytes that enable stable cycling for both the sulfurized polyacrylonitrile cathode and the Li anode.

SPAN was first synthesized in 2002 by heating a mixture of S and PAN at 300 °C (Wang et al.,[26] Figure 2b). When cycled in a carbonate-based electrolyte of 1 M $LiPF_6$ in EC:DMC (1:1, vol), SPAN delivered a reversible capacity of 780 mAh g^{-1}, with a 71% retention after 50 cycles. We note that the cycle number was obtained on a cell with a large excess of Li (same below unless otherwise noted). The historical application of carbonate electrolytes with this material is critical due to their incompatibility with liquid-phase PSs, which precludes their

https://doi.org/10.1021/acsenergylett.3c01711
ACS Energy Lett. 2023, 8, 4818−4830

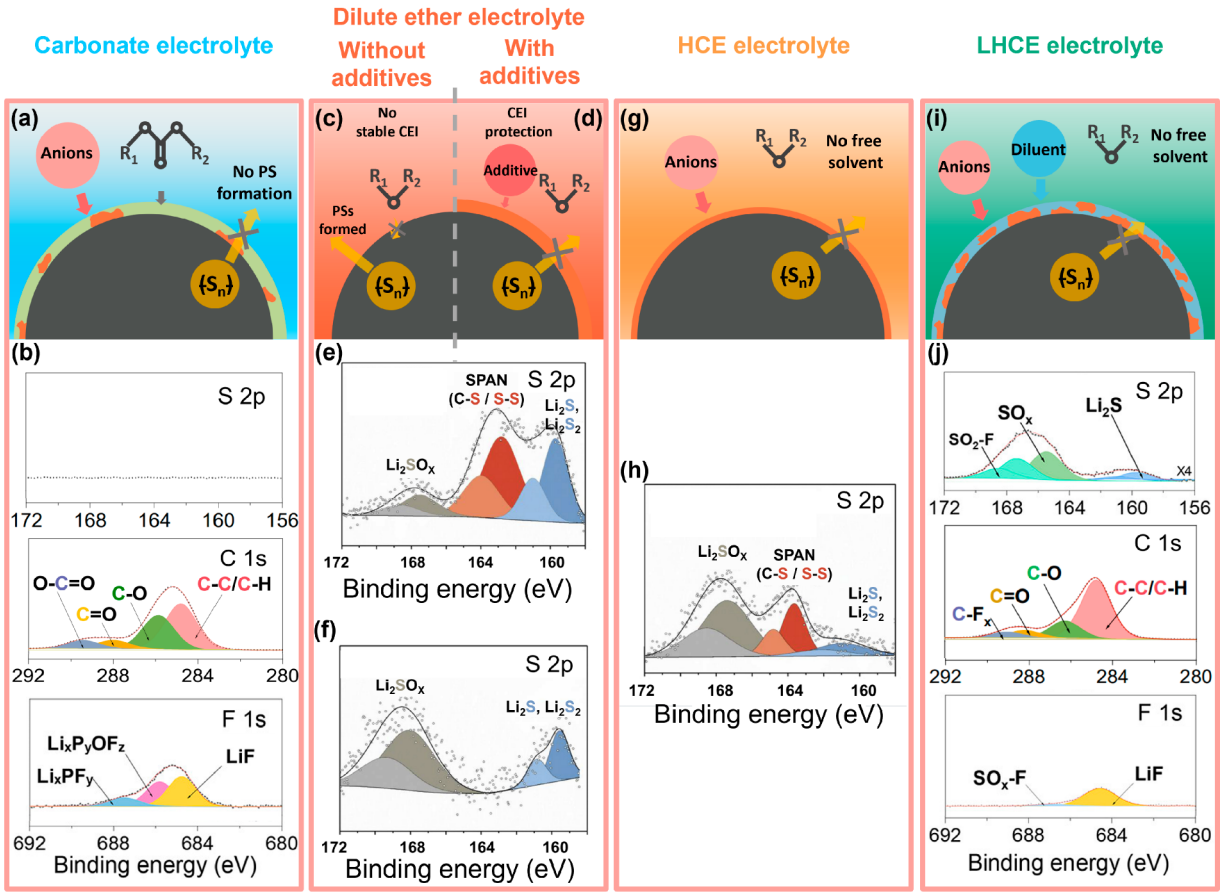

Figure 3. Impact of four families of electrolytes on the surface chemistry and the formation of the cathode−electrolyte interface on SPAN. (Top) Schematic diagrams for behavior of dilute carbonate electrolyte (a), dilute ether electrolyte without additives (c), dilute ether electrolyte with additives (d), high-concentration electrolyte (g), and localized high-concentration electrolyte (i) on SPAN cathodes. (Bottom) XPS results for SPAN cathodes after cycling in 1 M $LiPF_6$ in EC/EMC with VC additives (b), 1 M LiTFSI in DOL/DME (e), 1 M LiTFSI in DOL/DME with $LiNO_3$ (f), 4 M LiTFSI in DOL/DME, and LiFSI-1.2DME-3TTE (j). Panels b and j reproduced with permission from ref 43. Copyright 2022 American Chemical Society. Panels e, f, and h reproduced with permission from ref 44. Copyright 2019 Elsevier.

application in Li-S batteries based on elemental S. However, the solid−solid conversion mechanism inherent to SPAN enables their application.[27]

Unfortunately, the compatibility between carbonate electrolytes and SPAN is undercut by their incompatibility with Li metal, which cycles poorly due to the high reactivity of carbonates and their strong tendency to produce dendritic morphologies.[28] This also results in low Coulombic efficiency (CE) during plating and stripping. Modifications of salts or use of additives can be effective to address this incompatibility. For example, an electrolyte composed of 1 M LiDFOB/EC-DMC-FEC enabled a SPAN cell with excess Li to retain 89% of the capacity after 1100 cycles while delivering a plating and stripping CE of 98.8% in Li-Cu cells (Xu et al.,[29] Figure 2b). However, these approaches have yet to yield Li metal reversibility on par with what is necessary for practical Li metal cells (CE > 99.5%).

The concern for lithium cycling stability drove the community to explore the use of ether-based electrolytes, which feature significantly improved reductive stability. Unfortunately, a 2011 report (Fanous et al.,[30] Figure 2b) showed that a dilute ether electrolyte led to rapid capacity degradation due to the dissolution of PSs during cycling. The dilute ether electrolyte apparently returned the SPAN chemistry to one similar to that of elemental S, eliminating any potential advantages. To address this challenge, researchers drew inspiration from the advancements in electrolytes for elemental S cathodes, where $LiNO_3$ has been widely applied as an electrolyte additive to suppress the PS redox shuttle and to stabilize the Li metal anode.[31] Unfortunately, the application of additives such as $LiNO_3$, which are progressively consumed by the Li metal anode during cycling, renders their effects temporary.[32]

In search of a more permanent solution, researchers later reasoned that, since PSs can be regarded as salts, saturating the electrolyte with other lithium salts should discourage PS dissolution (referred to as the "common ion effect").[33] Applying this to SPAN, a HCE electrolyte, 5 M LiTFSI in DOL/DME, with $LiNO_3$ as the additive was shown to enable stable cycling of a S-rich SPAN electrode, with a retention rate of 71% after 100 cycles (Zhang et al.,[34] Figure 2b). Unfortunately, the continuous consumption of $LiNO_3$ limits practicality for long-term cycling. Consequently, decreasing the molecular polarity of solvents was explored as another way to lower PS solubility.[35] In 2018, SPAN in an electrolyte of 4 M LiFSI in dibutyl ether (DBE) demonstrated a 97% capacity

https://doi.org/10.1021/acsenergylett.3c01711
ACS Energy Lett. 2023, 8, 4818−4830

retention after 150 cycles (Zhou et al.,[36] Figure 2b). This composition was inspired by the low polarity of DBE as well as the identification of LiFSI as a key enabler for high-efficiency Li cycling, presumably due to its ability to promote the formation of LiF as an SEI component (Qian et al.,[28] Figure 2c). The DBE-based HCE electrolyte not only provides low solubility for PSs but also has a low reactivity with lithium.[36] Despite the chemical stability of the HCE electrolyte, the high salt concentration results in increased viscosity and decreased ionic conductivity, thus leading to severe transport issues.

The transport limitations of HCE systems are partially addressed by the advent of LHCE systems (Chen et al.,[37] Figure 2c). It was reported that, in 1.1 M LiFSI in TEP/TTE, SPAN shows a capacity retention of 92.4% after 100 cycles (Yang et al.,[38] Figure 2b). In 2021, another ether-based LHCE, 1.8 M LiFSI in DEE:BTFE (1:4, mass), enabled SPAN to cycle stably for 1200 cycles without capacity decay while achieving a lithium CE of 99.37% for 900 cycles in a Li-Cu cell (Liu et al.,[39] Figure 2b). The momentum of electrolyte development for Li-SPAN electrolytes has thus shifted significantly away from carbonates toward HCE and LHCE systems in recent years.[36,39] However, despite their relative transport and wetting improvements over HCEs, LHCEs are still insufficient in this arena once the loading and corresponding operating current density are increased. It has been recently demonstrated that, under such strenuous conditions, Li-SPAN cells fail due to shorting rather than capacity loss, with dendritic growth induced by transport limitations to blame (Wu et al.,[40] Figure 2b). Constant current cycling of a high areal loading electrode leads to a discharge time exceeding the Sand's time of the electrolyte, which is defined as the time when the surface Li^+ concentration approaches zero. This is consistent with the observation in 2016 that, once an electrode capacity exceeds the Sand's capacity (Sand's time × current applied), dendritic tip growth of lithium causes shorting for Li metal batteries (Bai et al.,[41] Figure 2c). These limitations fundamentally motivate the development of new Li-SPAN electrolytes, which is discussed later in this Review.

To provide guidelines for the development of next-generation electrolytes that enable long cycle life in Li-SPAN cells, it is first necessary to understand the fundamental significance and working mechanisms of previously developed and current electrolytes in enabling both the SPAN and Li metal electrodes to cycle stably.

IMPACT OF ELECTROLYTE ON THE SPAN CATHODE: THE CRITICAL ROLE OF THE CATHODE−ELECTROLYTE INTERFACE

To support stable SPAN cycling, the electrolyte must serve the following roles:

(1) *Suppression of PS dissolution.* Since the formation of PSs leads to sulfur loss and subsequent capacity degradation, it is vital to select an electrolyte that has low solubility for PSs and can suppress the rearrangement of -S_x- (x < 4) groups in SPAN.

(2) *Formation of a solid and conductive cathode−electrolyte interface (CEI).* The 80% volume change associated with S lithiation[1] and the necessary formation of PSs prevent the formation of a CEI layer on elemental sulfur cathodes. In contrast, SPAN displays a smaller volume change (22% thickness change for the electrode[42]) and does not have to generate soluble PSs to operate. A stable CEI has been suggested to further suppress PS dissolution and is associated with reversible performance.

The impact of the electrolyte on both PS dissolution and CEI formation is illustrated in Figure 3, where the schematics show the CEI structure on a SPAN particle surface, as well as the formation of the CEI and its interaction with the electrolytes. Also shown are the X-ray photoelectron spectroscopy (XPS) results obtained on the SPAN surface after cycling to identify the chemical species. In carbonate electrolytes, salts and carbonate solvents decompose on the surface of SPAN, forming a layer of CEI, thus preventing further irreversible reactions (Figure 3a). On the surface of cycled SPAN, the C 1s XPS spectrum (Figure 3b) shows the presence of $ROCO_2Li$ and $(-CH_2CH_2O-)_n$ species due to the nucleophilic reaction between carbonate and Li_2S_2, while the salt decomposition results in the formation of $Li_xP_yOF_z$ and LiF, as evidenced by the F 1s signals. Continued cycling appears to induce further growth of the organic portion of this CEI layer.[43]

In dilute ether electrolytes (Figure 3c), ethers are known to be stable toward PS species but are excellent solvents. As a result, lithiation of SPAN results in the formation of soluble long-chain PSs, or -S_x- (x > 4), in the liquid phase. There is no apparent CEI to prevent continuous dissolution. In 1 M LiTFSI in DOL/DME, the S 2p XPS spectrum of cycled SPAN (Figure 3e) shows a weak signal attributed to Li_2SO_x and strong signals from C−S bonds and S−S bonds attributed to SPAN itself, indicating that the surface is not covered with a stable CEI layer. Further, a discharge plateau at 2.1 V was observed in the voltage profile, a signature of PS redox (Figure S1).[44] SPAN thus resembles elemental S after the first cycle, suffering from the same shuttle effect and capacity degradation. Proper additives, e.g., $LiNO_3$, can promote the formation of a stable CEI (Figure 3d). After cycling in 1 M LiTFSI in DOL/DME with 0.5 M $LiNO_3$, the SPAN surface shows a clear presence of Li_2SO_x, as evidenced by the S 2p XPS spectrum (Figure 3f). More importantly, no signal from SPAN itself is observed, which indicates the existence of a CEI layer on the surface. Meanwhile, the discharge plateau at 2.1 V also disappears (Figure S1).[44] $LiNO_3$ oxidizes the sulfur species to Li_2SO_x, an important component of the CEI.[44] Another additive example is EC in 1 M LiFSI in DME,[45] which promotes the formation of a polycarbonate-rich CEI, effectively suppressing the PS dissolution in ether solvents. Since additives are consumed during cycling, ether solvents with low solubility of PSs, including DBE,[36] DEE,[46] DMM,[47] and DPE,[48] have been developed that have enabled promising cycling stability.

In HCE systems (Figure 3g), the increased salt/solvent ratio drives down the amount of free solvent molecules, which are largely recruited for Li^+ solvation. As a result, the CEI is mainly derived from the decomposition of the anions. The increased concentration of salts also helps to minimize the solubility of PSs. For example, on the surface of SPAN cycled in 4 M LiTFSI in DOL/DME, the S 2p XPS spectrum (Figure 3h) shows a prominent Li_2SO_x signal.[44] Li_2S_6 solubility also decreases with increasing concentration of Li salts. Both of these factors contribute to the better cycling stability compared to that of dilute ethers. However, XPS results also show signals from bulk SPAN, indicating that the CEI is too thin or incomplete to fully protect the cathode.

https://doi.org/10.1021/acsenergylett.3c01711
ACS Energy Lett. 2023, 8, 4818−4830

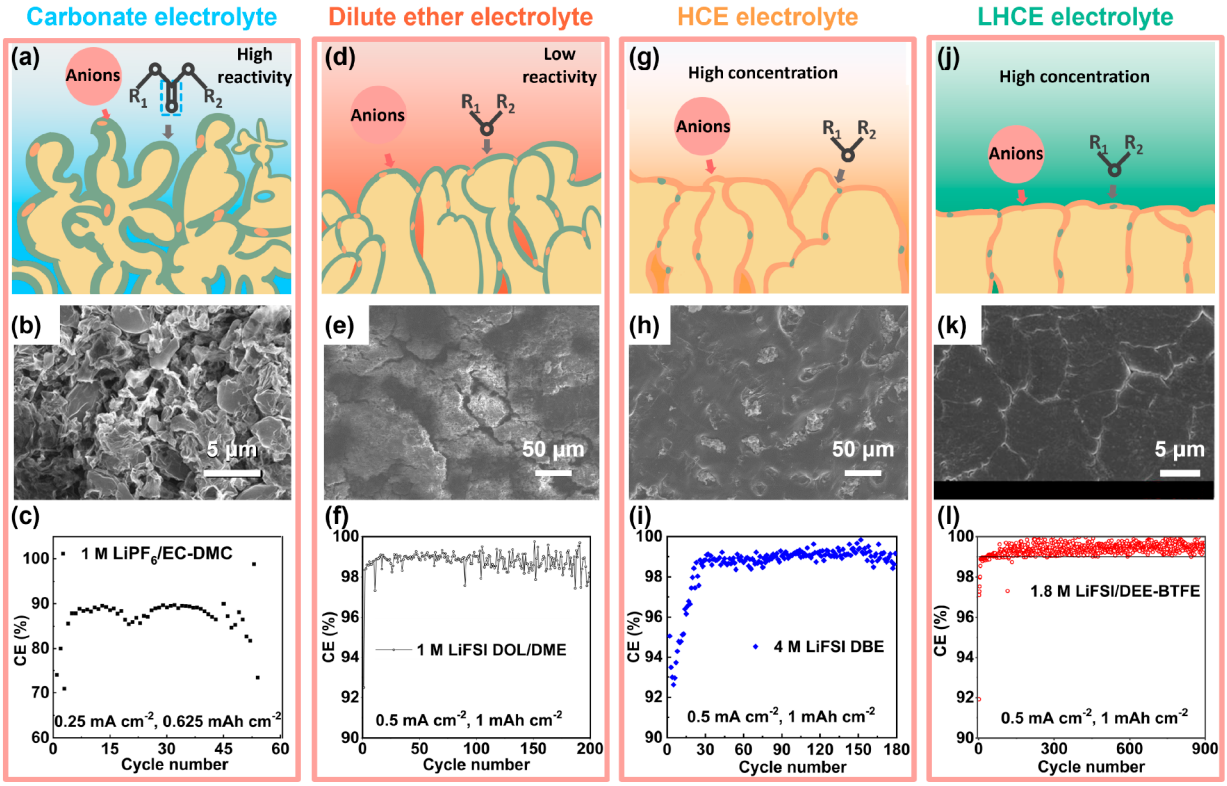

Figure 4. Impact of four types of electrolytes on the stability and SEI composition of a Li anode. (Top) Schematic diagrams for the behavior of dilute carbonate electrolyte (a), dilute ether electrolyte (d), high-concentration electrolyte (g), and localized high-concentration electrolyte (j) on Li anodes. (Middle) SEM images of Li anode morphologies from Li-SPAN cells after cycling in 1 M $LiPF_6$ in EC-DMC for 120 cycles (b), in 1 M LiFSI in DOL/DME for 50 cycles (e), in 4 M LiFSI in DBE for 50 cycles (h), and in 1.8 M LiFSI in DEE-BTFE for 62 cycles (k). (Bottom) Coulombic efficiency test results of Li-Cu cells in 1 M $LiPF_6$ in EC-DMC (c), 1 M LiFSI in DOL/DME (f), 4 M LiFSI in DBE (i), and 1.8 M LiFSI in DEE-BTFE (l). Panels b and c reproduced with permission from ref 13. Copyright 2018 Elsevier. Panels e, h, and i reproduced with permission from ref 36. Copyright 2018 Royal Society of Chemistry. Panels k and l reproduced with permission from ref 39. Copyright 2021 Elsevier. Panel f reproduced with permission from ref 46. Copyright 2021 Springer Nature.

In LHCE (Figure 3i), both the anion and the diluent contribute to the formation of a robust CEI. Since the diluent is highly fluorinated, it does not show solubility toward any lithium salts, including PSs. For example, on the surface of cycled SPAN in LiFSI:DME:TTE (1:1.2:3, mol), the S 2p XPS spectrum shows signals from SO_x and SO_2-F species, while the F 1s XPS spectrum shows signals from LiF and SO_x-F (Figure 3j).[43] AIMD simulations support the claim that TTE and LiFSI would decompose to form an inorganic-rich CEI on the SPAN surface, while DME is not a contributor due to its inherent stability. As a result, this electrolyte enables SPAN to show a capacity retention of 86.9% after 400 cycles.

IMPACT OF ELECTROLYTE ON THE FORMATION OF THE SOLID–ELECTROLYTE INTERFACE AND THE STABILITY OF THE LITHIUM METAL ANODE

To support stable Li cycling, the electrolyte must fulfill the following requirements:

(1) *Solvents need to have minimal reactivity with Li metal.* Corrosion reactions at the interface would not only induce dendrite growth but also cause severe electrolyte consumption during cycling.

(2) *Electrolytes need to promote the formation of stable solid–electrolyte interface (SEI) layers.* SEI layers are formed by the reduction of solvents and/or salts. They contain inorganic components such as LiF, Li_2O, and Li_2CO_3 and organic species such as $ROCO_2Li$, Li alkoxides, and Li alkylcarbonates.[49] While a consensus for the composition and microstructure of an "ideal" SEI remains elusive, it is generally accepted that high ionic conductivity, low electronic conductivity, low solvent permeability, and high mechanical toughness are highly desirable.[49] As a result, it is claimed that a stable inorganic-rich and thin SEI layer is highly desirable to maintain Li anode stability.[49]

(3) *Electrolytes should provide sufficient rates of ion transport under operating conditions.* During Li deposition, Li ions are consumed at the interface. Once the plating capacity exceeds the Sand's capacity, the local depletion of Li ions triggers Li dendrite growth.

The impact of electrolyte design on Li morphology and cycling stability is illustrated in Figure 4. In keeping with the literature, we estimate the inherent electrochemical stability of a given electrolyte vs Li metal (criteria 1 and 2 above) through CE values obtained from cycling tests in Li-Cu cells, which in turn dictate the Li inventory loss during cycling and cycle life at the full cell level. In dilute carbonate electrolytes (Figure 4a), it is well established that typical carbonate solvents are reductively unstable, and their reduction results in the formation of an organic-rich SEI layer. These SEI layers do not effectively protect the Li anode from further side reactions,

https://doi.org/10.1021/acsenergylett.3c01711
ACS Energy Lett. 2023, 8, 4818−4830

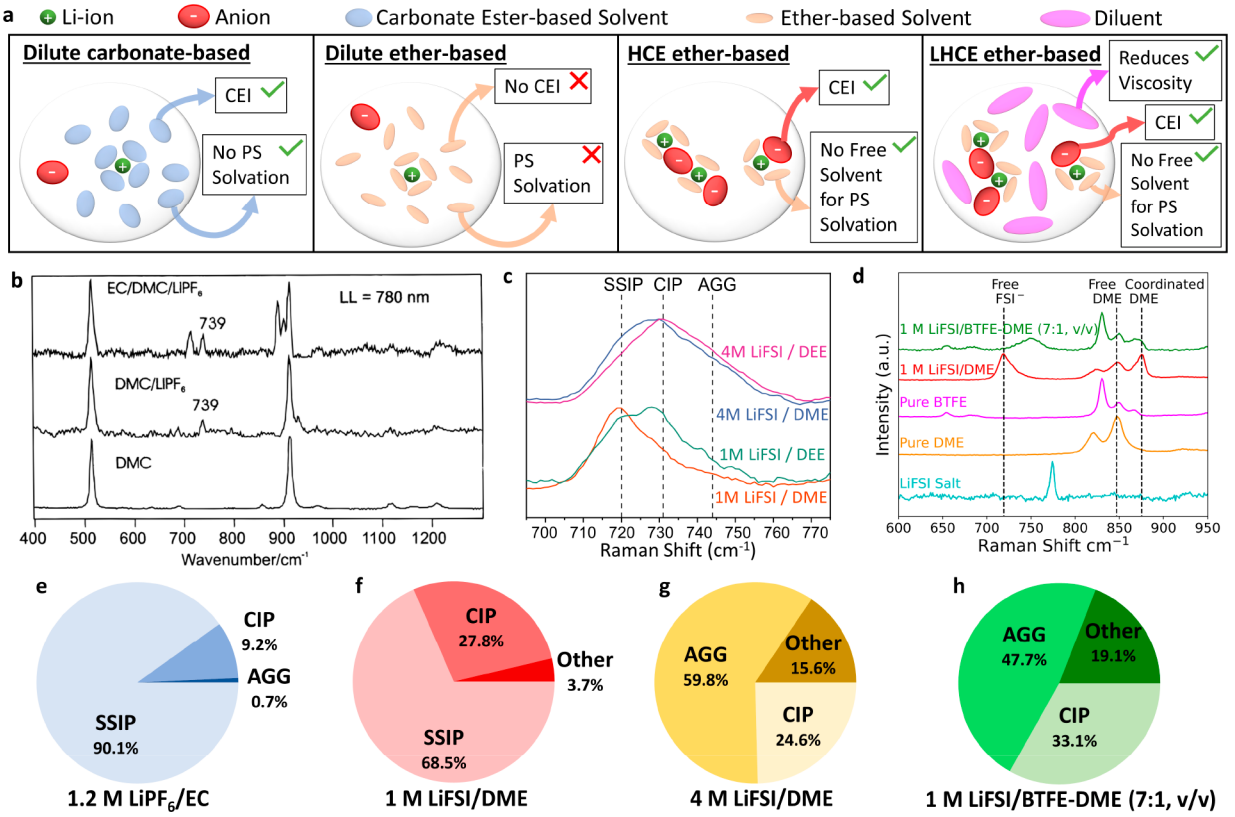

Figure 5. Solvation structures of the various electrolytes. (a) Schematic diagram of the general solvation structures of the four electrolytes and their impacts on CEI formation, PS solvation, and viscosity. (b) Raman spectra of neat DMC, 1 M $LiPF_6$ in DMC, and 1 M $LiPF_6$ in EC/DMC. (c) Raman spectra of 1 and 4 M LiFSI in DME and DEE. We note that the DEE used here refers to 1,2-diethoxyethane, not diethyl ether. (d) Raman spectra of LiFSI in BTFE-DME (7:1, v/v), 1 M LiFSI in DME, and the various electrolyte components. (e–h) Solvation structure compositions, obtained through MD simulations, of 1.2 M $LiPF_6$ in EC (e), 1 M LiFSI in DME (f), 4 M LiFSI in DME (g), and 1 M LiFSI in BTFE-DME (7:1, v/v) (h). Panel b reproduced with permission from ref 53. Copyright 2000 Springer Nature. Panels c and g reproduced with permission from ref 57. Copyright 2021 American Chemical Society. Panels d, f, and h reproduced with permission from ref 58. Copyright 2022 Royal Society of Chemistry. Panel e reproduced with permission from ref 55. Copyright 2021 Royal Society of Chemistry.

leading to dendrite growth and lithium with high porosity.[28] The Li anode in a Li-SPAN cell cycled in 1 M $LiPF_6$ in EC/DMC (1:1) (Figure 4b) shows severe dendrite growth and pulverization after 120 cycles.[13] A corresponding Li-Cu cell test also shows a low average CE of 74.1% for 150 cycles (Figure 4c).[13] The poor Li metal compatibility severely restricts its application in Li-SPAN batteries. Improving the SEI by changing the salt and using additives can be effective. As mentioned above, the synergistic effect of LiDFOB and FEC results in the formation of a SEI which integrates the rigid LiF and flexible organic components, effectively protecting lithium from further side reactions with the electrolyte.[29] In another example, lithium cycled in 1 M LiFSI in EMC/FEC (7:3, vol) shows a LiF-rich SEI due to the decomposition of LiFSI and FEC.[13] The Li morphology is significantly improved, and the average CE is improved to 96% for 150 cycles in a Li-Cu cell.[13]

In dilute ether electrolytes (Figure 4d), the low reactivity of ether solvents generally results in a less dendritic Li morphology, along with an SEI that is more derived from salt reduction.[50−52] In a typical electrolyte of 1 M LiFSI in DOL/DME (1:1, vol), a mostly dendrite-free morphology is observed for the Li anode (Figure 4e) after 50 cycles in a Li-SPAN cell.[36] In this dilute ether electrolyte, an average CE of 98.76% over 200 cycles is obtained in a Li-Cu cell (Figure 4f).[46] Li cycled in 1 M LiFSI in DEE shows an even higher CE of 99.18% over 200 cycles, likely due to the even lower reactivity of DEE than DME toward Li metal.[46]

In HCE electrolytes (Figure 4g), ether solvents are bonded to lithium ions, which promote the formation of a SEI dominated by salt-derived species. The porosity of electrodeposited Li is also reported to be lower as compared to that with dilute ether electrolytes under the same conditions.[28] For example, a uniform, dendrite-free Li morphology is observed (Figure 4h) in 4 M LiFSI in DBE after 50 cycles when tested in a Li-SPAN cell (Figure 4i).[36] An average CE of 99.2% is obtained for 60 cycles, while the CE of 1 M LiFSI in DBE drops to 20% in 20 cycles (Figure 4i).[36] In the 4 M LiFSI-ether electrolyte, the SEI layer is reported to be mainly formed due to the reaction between Li and anions rather than the solvent decomposition, leading to a low Li ion transport resistance, thus contributing to the high CE and uniform Li deposition morphology.[28]

In LHCE systems (Figure 4j), the non-solvating diluents not only reduce the concentration of reactive species on the Li surface but also further promote the reaction between Li and anions to suppress the side reaction with solvents.[52] Several reports indicate that Li deposited in LHCE systems typically has lower porosities than in HCE systems under similar deposition conditions.[50,52] As a result, LHCE systems

https://doi.org/10.1021/acsenergylett.3c01711
ACS Energy Lett. 2023, 8, 4818−4830

demonstrate enhanced Li compatibility. For example, in 1.8 M LiFSI in DEE/BTFE (1:4, mass), dense Li deposition is maintained after 62 cycles in a SPAN cell (Figure 3k), along with a high CE of 99.37% for over 900 cycles (Figure 4l).[39]

MOLECULAR ORIGINS OF ELECTROLYTE PERFORMANCE

The ability of the electrolytes to promote the formation of stable SEI and CEI layers is determined by the stability of the salts, solvents, and additives. A crucial consideration is the solvation structure, or how the solvent molecules interact with the ions. There are three main solvation environments surrounding the Li^+ ions that are of interest: solvent-separated ion pairs (SSIPs), contact-ion pairs (CIPs), and aggregates (AGGs). In SSIP solvation structures, the Li^+ ions are exclusively coordinated by solvent molecules with no ion-pairing. In CIP solvation structures, the cation is coordinated with a singular anion, in addition to the solvent. In AGG solvation structures, the cations coordinate with multiple anions, and the anions coordinate with multiple cations, forming ion aggregates. As the Li^+ ions are transported from the bulk electrolyte to an electrode surface, the solvation sheath is dragged by the Li^+ ions toward the interface, resulting in an intrinsic relationship between the solvation structure and the interphasial chemistry. Figure 5a visualizes the representative solvation structures and their ability to form CEI layers on SPAN surfaces for the four classes of electrolytes of interest. Solvation structures have been commonly investigated by Raman spectroscopy supported by molecular dynamics (MD) simulations.

In dilute carbonate-based electrolytes, the dominate Li^+ ion solvation structure is believed to be SSIP. Raman spectra for 1 M $LiPF_6$ in EC/DMC and 1 M $LiPF_6$ in DMC are seen in Figure 5b.[53] The totally symmetric vibrational mode of the PF_6^- anion, seen at 745 cm^{-1} for the $LiPF_6$ salt, shifts to 739 cm^{-1} in the carbonate electrolytes. This indicates that there is some ion-pairing; however, the degree of ion-pairing is unclear. Furthermore, Raman spectroscopy is seen to be troublesome for carbonate electrolytes due to the difficulty of deconvoluting the overlapping bands of differing carbonates, as well as the inability to distinguish between SSIP and CIP solvation structures when $LiPF_6$ is the salt.[54] Therefore, computation is helpful to provide more insights. From MD simulations performed on 1.2 M $LiPF_6$ in EC,[55] it is calculated that the vast majority of solvation structures are SSIPs (90.1%), with the remainder comprised mostly of CIPs (Figure 5e). Due to the SSIP solvation structure of carbonate-based electrolytes, the CEI and SEI are subsequently composed primarily of degraded carbonate solvents (Figure 5a). The CEI at the SPAN surface is formed by the nucleophilic sulfide groups of SPAN reacting with the carbonate solvents to form thiocarbonate and thioether groups.[23] The covalent bonds between the sulfur and the carbon backbone in SPAN prevent PS solvation. At the Li-metal anode, the LUMO energy level of carbonate solvents is much lower than the corresponding energy level of the Li^+/Li electrode potential, resulting in carbonates having a low reductive stability.[56] Therefore, the SEI arises due to the reduction of the carbonate solvent molecules by Li^0. However, the high reactivity of Li metal with carbonates, combined with new deposition of Li metal during each cycle, causes the SEI to become uneven and inhomogeneous (Figure 4a). For this reason, carbonate solvents are found to be incompatible with Li metal anodes.

Dilute ether electrolytes are also dominated by SSIP solvation structures. This is often observed qualitatively through Raman measurements (Figure 5c).[57] The vibrational nodes of the FSI^- anion result in three convoluted peaks between 710 and 760 cm^{-1}, corresponding to SSIP, CIP, and AGG solvation structures. For 1 M LiFSI in DME, there is a major peak at 720 cm^{-1}, indicating a predominantly SSIP solvation structure. MD simulations provide a quantitative verification of these results (Figure 5f), as 68.5% of the coordination environments were calculated to be SSIP.[58] The majority SSIP solvation structure results in the interphases at electrode surfaces being primarily composed of solvent derivatives, similar to carbonate electrolytes. In contrast to carbonate electrolytes, ethers such as DOL and DME have LUMOs at higher energies than the Li^+/Li electrode potential, allowing a greater reductive stability.[56] This leads to a thinner and less resistive SEI that can better support the cycled deposition and stripping of lithium metal (Figure 4b). However, the high reductive stability of ethers also prevents the nucleophilic sulfide groups of SPAN from reacting with ethers and forming a CEI. The lack of a CEI gives opportunities for PS formation and solvation, leading to detrimental PS shuttling (Figure 5a). Introducing $LiNO_3$ as an additive in dilute ethers helps circumvent the PS issue as, NO_3^- anions become reduced at the electrode interfaces to help form a stable CEI and SEI, effectively suppressing PS dissolution.[44]

For ether-based HCEs, Li^+ ions largely have CIP and AGG coordination environments. This is well illustrated by the Raman spectra of 4 M LiFSI in DME (Figure 5c).[57] The large emergence of CIP and AGG solvation structures in HCE ethers was also noted by MD simulations, as AGGs made up 59.8% and CIPs made up 24.6% of the coordination environments for 4 M LiFSI in DME (Figure 5g).[57] The high concentration of anions in the solvation structures led to a higher activity of the anion, making the anions more readily decomposed to form the SEI and CEI. We also note that there is very little presence of any free solvent molecules, as the solvent molecules are tightly coordinated to the ions, as shown in Raman studies by Zhang et al.[59] The absence of free ether solvent molecules helps prevent PS solvation but greatly increases the viscosity of the electrolyte. Furthermore, the strong Coulombic pairing between ions significantly reduces the diffusivity of the ions. The increase in viscosity and decrease in ionic diffusivity are reflected in a stark decrease in the ionic conductivity of HCE ethers compared to dilute ether electrolytes (Figure S2). We note that the use of weakly solvating solvents such as DEE can promote the formation of CIP solvation structures, even in dilute electrolytes. However, they suffer from a similar reduction in ionic conductivity (Figure S2).

In LHCE ethers, the solvation structure of HCE ethers is preserved, which again consist mostly of CIPs and AGGs. This is corroborated by the Raman spectrum for the ether-based LHCE, 1 M LiFSI in BTFE-DME (7:1, v/v) (Figure 5d).[58] The peak corresponding to free FSI^- anions is shown to shift from 719 cm^{-1} in 1 M LiFSI in DME to 748 cm^{-1} in the LHCE. The peak shifts closer to that of the LiFSI salt, indicative of an increase in ion-pairing and, therefore, the presence of CIP and AGG solvation structures. MD simulations further indicate the dominance of AGG and CIP in the composition of LHCE coordination environments (Figure 5h).[58] Similar to HCEs, the SEI and CEI are formed

https://doi.org/10.1021/acsenergylett.3c01711
ACS Energy Lett. 2023, 8, 4818−4830

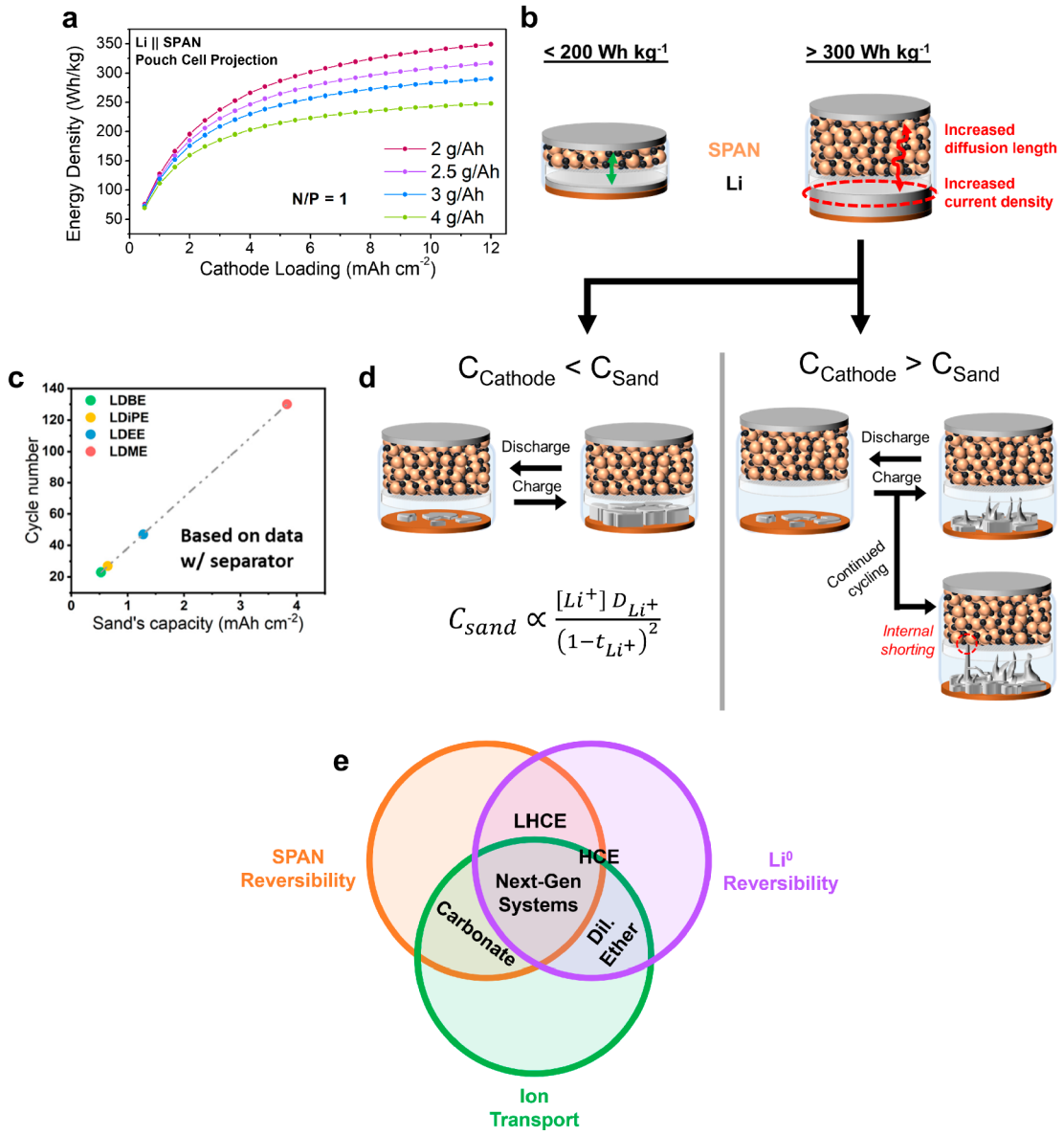

Figure 6. Electrolyte design requirements imposed by practical Li-SPAN batteries. (a) Pouch-cell-level energy density projections of Li-SPAN batteries at N/P = 1 as a function of cathode and electrolyte loading. (b) Schematic representation of the relationship between high energy density and the transport penalty placed on the electrolyte. (c) Correlation between Li-SPAN battery shorting and the Sand's capacity of the electrolyte. (Reproduced with permission from ref 40. Copyright 2022 American Chemical Society.) (d) Schematic representation of shorting-induced failure of Li-SPAN cells as a result of sufficient and insufficient Li^+ transport. (e) Summary of current electrolytes with respect to the three main electrolyte requirements of practical Li-SPAN batteries. The development of next-generation systems must simultaneously satisfy all three requirements.

predominantly by the decomposition of the anions, and there is again very little free solvent for PS solvation. The main difference is the presence of diluents outside the Li^+ ion solvation sheath that reduces the bulk viscosity of the electrolyte. Highly fluorinated ethers, such as BTFE, are common choices for diluents. The presence of many fluorines draws the electron availability away from the oxygen, resulting in an effectively nonpolar molecule. The lack of polarity renders these highly fluorinated ethers unable to solvate Li^+ ions, resulting in no influence in the solvation structures.[60] This is reflected in the Raman spectra for 1 M LiFSI in BTFE-DME (7:1, v/v), as there is no significant change in the major peak corresponding to pure BTFE.[58] Using a solvent with a weaker solvating power, such as DMP, can further increase the number of AGG solvation structures in LHCEs and promote a higher concentration of anion-derived species in the interphases.[61] However, despite the improved viscosity, the ionic conductivities of LHCE ethers are still low due to the presence of ion pairing, as well as the lower salt concentration compared to HCE ethers (Figure S2).

Li-SPAN ELECTROLYTE DEVELOPMENT OUTLOOK

Despite the high capacity of SPAN, its low voltage relative to those of transition metal oxide cathodes inherently requires elevated cathode loading to reach similar cell-level energy densities. At a N/P ratio of 1, and with a commercially lean electrolyte of 2.5 g Ah^{-1}, we project that capacity loadings >8.5 mAh cm^{-2} (>12.1 mg cm^{-2} at 700 mAh g^{-1}) are necessary to

https://doi.org/10.1021/acsenergylett.3c01711
ACS Energy Lett. 2023, 8, 4818−4830

exceed 300 Wh kg^{-1} at the pouch cell level (Figure 6a). To achieve the C-rates necessary for device operation, such elevated loadings directly translate to elevated current densities applied on the Li anode. These elevated current densities, in turn, place an increased Li^+ transport burden on the electrolyte (Figure 6b). This burden is further compounded by the increased tortuosity and diffusion distance inherent to increased cathode thickness.

While insufficient Li^+ transport in the bulk electrolyte may negatively affect the polarization and capacity utilization of the cathode, its effects on the Li anode are far more catastrophic. A critical concept when discussing such limitations is the "Sand's time", at which the surface concentration of the reactant ion becomes zero, which is directly proportional to the concentration and diffusion coefficient of Li^+ and is inversely proportional to $1 - t_{Li^+}$.[62] Bai et al. demonstrated that, at this juncture, a distinct transition occurs in the growth of Li metal toward a heavily dendritic regime, which raises concerns of internal shorting for such Li metal cells.[41] Indeed, our recent work with high-loading Li-SPAN batteries indicated not only that shorting is the primary source of failure for such cells but also that the cycle at which the short first occurs is directly correlated with the Sand's time of the electrolyte in question (Figure 6c).[40] This effect was observed in LHCE systems of various compositions with comparable high CE values for Li anode cycling and limited capacity degradation for SPAN cycling. We proposed that this heavy correlation is a direct product of the *time spent in each cycle* > *Sand's time* (or capacity continuously passed > Sand's capacity), which compounds over the cycle life of the cell, eventually producing a short (Figure 6d). The somewhat grim implication of this model, however, is that any cell operating beyond the Sand's limit regularly is doomed to fail, regardless of the lab-scale reversibility of Li and SPAN endowed by the electrolyte of interest.

Improving the viability of practical, high-energy Li-SPAN cells relies on improving the transport properties of the electrolyte while maintaining the cells' ability to ensure Li and SPAN reversibility.

Improving the viability of practical, high-energy Li-SPAN cells therefore relies on improving the mass transport of Li^+ in the electrolyte while maintaining the aforementioned inherent Li and SPAN reversibility. While simultaneously maximizing the ionic conductivity (proportional to D_{Li^+} in a dilute solution), salt concentration, and t_{Li^+} is necessary to enhance Sand's time/capacity, these characteristics are often at odds in practical systems. For example, the heavy ion-pairing and elevated viscosity of HCE systems depresses their ionic conductivity, neutralizing the ostensible benefits of their increased salt concentration and t_{Li^+}. Moreover, achieving improved Sand's time/capacity in an electrolyte while maintaining or improving Li anode and SPAN cathode reversibility adds another layer of complexity to the exercise. Considering the current state-of-the-art, the heavily ion-paired structures found in HCE and LHCE systems give rise to stable SEI and CEI compositions but inherently reduce the overall ionicity and diffusion coefficient for Li^+ in the system (Figure 6e).

To achieve both improved Li^+ transport and improved nascent Li-SPAN reversibility, fundamental advances in electrolyte design are therefore necessary. We propose that several targeted research efforts can and should be aimed at this challenge. First, the development of advanced additives to enable the stable cycling of SPAN and enhance the Li anode reversibility of conventional ether electrolytes could take full advantage of their inherently superior ionic conductivity. While $LiNO_3$ ostensibly serves this role, its progressive consumption by the Li anode renders its effects temporary.[32] Second, reducing the conductivity penalty encountered by conventional high-concentration electrolytes would be a promising route to maximize Sand's time/capacity to exploit the intrinsically high salt concentration while dampening the loss in D_{Li^+}. This could be through the development of reduced viscosity, strongly solvating HCEs to maximize ionicity, and wetting, which would require the investigation of new solvents or salts with weak self-association. Alternatively, "medium" (e.g., 2−5 M) concentration systems without significant polysulfide solubility and stable Li anode performance could be considered. Third, the development of next-generation LHCE systems designed to accelerate the transport of ion-paired structures is a promising avenue which maintains all the intrinsic Li and SPAN compatibility of LHCEs while improving Sand's time/capacity. Preliminary results from Kim et al. suggest that this is achievable via the "cocktail" effect, where the addition of multiple solvating agents generates a high solvation entropy, reducing local salt aggregation.[63] Finally, we note that there is intensive ongoing effort in developing SPAN with higher sulfur contents and higher capacities, which may introduce new electrochemical processes challenging the existing electrolyte chemistries. Regardless of the approach, the advent of next-generation Li-SPAN battery electrolytes necessitates the development of new electrolyte chemistries and/or design strategies.

■ ASSOCIATED CONTENT

Supporting Information

The Supporting Information is available free of charge at https://pubs.acs.org/doi/10.1021/acsenergylett.3c01711.

Table S1, a literature summary for Li-SPAN batteries; Figure S1, electrochemical curves for Li-SPAN; and Figure S2, an ionic conductivity summary for various electrolytes (PDF)

■ AUTHOR INFORMATION

Corresponding Authors

John Holoubek − *Department of Nanoengineering, University of California San Diego, La Jolla, California 92093, United States;* orcid.org/0000-0003-0015-4512; Email: jholoube@ucsd.edu

Ping Liu − *Program of Materials Science and Engineering, University of California San Diego, La Jolla, California 92093, United States; Department of Nanoengineering, University of California San Diego, La Jolla, California 92093, United States;* orcid.org/0000-0002-1488-1668; Email: piliu@ucsd.edu

Authors

Qiushi Miao − *Program of Materials Science and Engineering, University of California San Diego, La Jolla, California 92093, United States*

Nicholas Solan − *Department of Nanoengineering, University of California San Diego, La Jolla, California 92093, United States;* orcid.org/0009-0007-8884-4249

Gayea Hyun − *Department of Nanoengineering, University of California San Diego, La Jolla, California 92093, United States*

Complete contact information is available at: https://pubs.acs.org/10.1021/acsenergylett.3c01711

Author Contributions

[+]Q.M. and N.S. contributed equally to this work. P.L. and J.H. conceived the Review and directed the project. Q.M. and N.S. collected and analyzed the literature. G.H. conceived and created Figure 1. Q.M., N.S., J.H., and P.L. wrote the draft. All authors commented on the paper.

Notes

The authors declare no competing financial interest.

Biographies

Qiushi Miao is presently a Ph.D. student in the Program of Materials Science and Engineering at the University of California San Diego, under the supervision of Prof. Ping Liu. His research has focused on the electrochemical studies of lithium−sulfur batteries.

Nicholas Solan is currently a Ph.D. student in the Department of NanoEngineering at the University of California San Diego, under the supervision of Profs. Ping Liu and Tod Pascal. His research focuses on the development of liquid electrolytes for lithium batteries using a combined computational and experimental approach.

Gayea Hyun received her Ph.D. from the Korea Advanced Institute of Science and Technology in 2021. She is currently a postdoctoral researcher at the University of California San Diego, under the guidance of Prof. Ping Liu. Her research is focused on electrolytes and electrode materials for high-energy-density batteries.

John Holoubek received his Ph.D. from the University of California San Diego in 2023 under the supervision of Profs. Ping Liu and Zheng Chen. His research concerns the understanding of the molecular structure and electrochemistry of liquid electrolytes as well as the development of batteries capable of operating under extreme conditions.

Ping Liu is a professor of nanoengineering and the Director of the Sustainable Power and Energy Center at the University of California San Diego. Previously, he served as a Program Director at ARPA-E, a research manager at HRL Laboratories, and a research staff member at NREL. Prof. Liu received his Ph.D. in chemistry from Fudan University in China. His group studies materials and chemistry for batteries and fuel cells. https://liugroup.ucsd.edu

■ ACKNOWLEDGMENTS

This work was supported by the Office of Vehicle Technologies of the U.S. Department of Energy through the Advanced Battery Materials Research (BMR) Program (Battery500 Consortium) under Contract No. PNNL-595241.

■ ABBREVIATIONS

BTFE, Bis(2,2,2-trifluoroethyl) ether; DBE, Dibutyl ether; DEE, Diethyl ether; DMC, Dimethyl carbonate; DME, Dimethyl ether; DMM, Dimethoxymethane; DMP, 1,3-Dimethoxypropane; DOL, Dioxolane; DPE, Dipropyl ether; EC, Ethylene carbonate; FEC, Fluoroethylene carbonate; LiDFOB, Lithium difluoro(oxalato)borate; LiFSI, Lithium bis(fluorosulfonyl)imide; LiTFSI, Lithium bis-(trifluoromethanesulfonyl)imide; TEP, Triethyl phosphate; TTE, 1,1,2,2-Tetrafluoroethyl 2,2,3,3-tetrafluoropropyl ether

■ REFERENCES

(1) Manthiram, A.; Fu, Y.; Chung, S.-H.; Zu, C.; Su, Y.-S. Rechargeable Lithium-Sulfur Batteries. *Chem. Rev.* **2014**, *114* (23), 11751−11787.

(2) Manthiram, A.; Chung, S.-H.; Zu, C. Lithium-Sulfur Batteries: Progress and Prospects. *Adv. Mater.* **2015**, *27* (12), 1980−2006.

(3) He, Y.; Bi, S.; Jiang, C.; Song, J. Recent progress of sulfur cathodes and other components for flexible lithium-sulfur batteries. *Mater. Today Sustainability* **2022**, *19*, 100181.

(4) Manthiram, A.; Fu, Y.; Su, Y.-S. Challenges and Prospects of Lithium-Sulfur Batteries. *Acc. Chem. Res.* **2013**, *46* (5), 1125−1134.

(5) Shi, L.; Bak, S.-M.; Shadike, Z.; Wang, C.; Niu, C.; Northrup, P.; Lee, H.; Baranovskiy, A. Y.; Anderson, C. S.; Qin, J.; et al. Reaction heterogeneity in practical high-energy lithium-sulfur pouch cells. *Energy Environ. Sci.* **2020**, *13* (10), 3620−3632.

(6) Zhang, X.; Ma, H.; Liu, J.; Chen, J.; Lu, H.; Huang, Y.; Wang, J. Structure and reactions mechanism of sulfurized polyacrylonitrile as cathodes for rechargeable Li-S batteries. *Nano Res.* **2023**, *16* (6), 8159−8172.

(7) Wang, S.; Lu, B.; Cheng, D.; Wu, Z.; Feng, S.; Zhang, M.; Li, W.; Miao, Q.; Patel, M.; Feng, J.; et al. Structural Transformation in a Sulfurized Polymer Cathode to Enable Long-Life Rechargeable Lithium-Sulfur Batteries. *J. Am. Chem. Soc.* **2023**, *145* (17), 9624−9633.

(8) Fu, Y.; Manthiram, A. Core-shell structured sulfur-polypyrrole composite cathodes for lithium-sulfur batteries. *RSC Adv.* **2012**, *2* (14), 5927−5929.

(9) Choi, S.; Yoon, I.; Nichols, W. T.; Shin, D. Carbon-coated Li2S cathode for improving the electrochemical properties of an all-solid-state lithium-sulfur battery using Li2S-P2S5 solid electrolyte. *Ceram. Int.* **2018**, *44* (7), 7450−7453.

(10) Mentbayeva, A.; Belgibayeva, A.; Umirov, N.; Zhang, Y.; Taniguchi, I.; Kurmanbayeva, I.; Bakenov, Z. High performance freestanding composite cathode for lithium-sulfur batteries. *Electrochim. Acta* **2016**, *217*, 242−248.

(11) Kim, H. M.; Hwang, J.-Y.; Aurbach, D.; Sun, Y.-K. Electrochemical Properties of Sulfurized-Polyacrylonitrile Cathode for Lithium-Sulfur Batteries: Effect of Polyacrylic Acid Binder and Fluoroethylene Carbonate Additive. *J. Phys. Chem. Lett.* **2017**, *8* (21), 5331−5337.

(12) Yang, H.; Chen, J.; Yang, J.; Nuli, Y.; Wang, J. Dense and high loading sulfurized pyrolyzed poly (acrylonitrile)(S@pPAN) cathode for rechargeable lithium batteries. *Energy Storage Mater.* **2020**, *31*, 187−194.

(13) Chen, Z.; Zhou, J.; Guo, Y.; Liang, C.; Yang, J.; Wang, J.; Nuli, Y. A compatible carbonate electrolyte with lithium anode for high performance lithium sulfur battery. *Electrochim. Acta* **2018**, *282*, 555−562.

(14) Yang, X.; Li, X.; Adair, K.; Zhang, H.; Sun, X. Structural Design of Lithium-Sulfur Batteries: From Fundamental Research to Practical Application. *Electrochem. Energy Rev.* **2018**, *1* (3), 239−293.

(15) Yang, H.; Qiao, Y.; Chang, Z.; He, P.; Zhou, H. Designing Cation-Solvent Fully Coordinated Electrolyte for High-Energy-Density Lithium-Sulfur Full Cell Based On Solid-Solid Conversion. *Angew. Chem., Int. Ed.* **2021**, *60* (32), 17726−17734.

(16) Liu, H.; Yue, X.; Xing, X.; Yan, Q.; Huang, J.; Petrova, V.; Zhou, H.; Liu, P. A scalable 3D lithium metal anode. *Energy Storage Mater.* **2019**, *16*, 505−511.

(17) Yu, S.; Wu, Z.; Holoubek, J.; Liu, H.; Hopkins, E.; Xiao, Y.; Xing, X.; Lee, M. H.; Liu, P. A Fiber-Based 3D Lithium Host for Lean Electrolyte Lithium Metal Batteries. *Adv. Sci.* **2022**, *9* (10), 2104829.

(18) Zhou, H.; Liu, H.; Li, Y.; Yue, X.; Wang, X.; Gonzalez, M.; Meng, Y. S.; Liu, P. In situ formed polymer gel electrolytes for lithium batteries with inherent thermal shutdown safety features. *J. Mater. Chem. A* **2019**, *7* (28), 16984−16991.
(19) Liu, H.; Zhou, H.; Lee, B.-S.; Xing, X.; Gonzalez, M.; Liu, P. Suppressing Lithium Dendrite Growth with a Single-Component Coating. *ACS Appl. Mater. Interfaces* **2017**, *9* (36), 30635−30642.
(20) Wu, Z.; Wang, C.; Hui, Z.; Liu, H.; Wang, S.; Yu, S.; Xing, X.; Holoubek, J.; Miao, Q.; Xin, H. L.; Liu, P. Growing single-crystalline seeds on lithiophobic substrates to enable fast-charging lithium-metal batteries. *Nat. Energy* **2023**, *8* (4), 340−350.
(21) Chen, W.-J.; Li, B.-Q.; Zhao, C.-X.; Zhao, M.; Yuan, T.-Q.; Sun, R.-C.; Huang, J.-Q.; Zhang, Q. Electrolyte Regulation towards Stable Lithium-Metal Anodes in Lithium-Sulfur Batteries with Sulfurized Polyacrylonitrile Cathodes. *Angew. Chem., Int. Ed.* **2020**, *59* (27), 10732−10745.
(22) Zhao, X.; Wang, C.; Li, Z.; Hu, X.; Abdul Razzaq, A.; Deng, Z. Sulfurized polyacrylonitrile for high-performance lithium sulfur batteries: advances and prospects. *J. Mater. Chem. A* **2021**, *9* (35), 19282−19297.
(23) Ahmed, M. S.; Lee, S.; Agostini, M.; Jeong, M.-G.; Jung, H.-G.; Ming, J.; Sun, Y.-K.; Kim, J.; Hwang, J.-Y. Multiscale Understanding of Covalently Fixed Sulfur-Polyacrylonitrile Composite as Advanced Cathode for Metal-Sulfur Batteries. *Adv. Sci.* **2021**, *8* (21), 2101123.
(24) Jiang, G.; Li, F.; Wang, H.; Wu, M.; Qi, S.; Liu, X.; Yang, S.; Ma, J. Perspective on High-Concentration Electrolytes for Lithium Metal Batteries. *Small Struct.* **2021**, *2* (5), 2000122.
(25) Cao, X.; Jia, H.; Xu, W.; Zhang, J.-G. Review—Localized High-Concentration Electrolytes for Lithium Batteries. *J. Electrochem. Soc.* **2021**, *168* (1), 010522.
(26) Wang, J.; Yang, J.; Xie, J.; Xu, N. A Novel Conductive Polymer-Sulfur Composite Cathode Material for Rechargeable Lithium Batteries. *Adv. Mater.* **2002**, *14* (13−14), 963−965.
(27) Zhang, S. S. Understanding of Sulfurized Polyacrylonitrile for Superior Performance Lithium/Sulfur Battery. *Energies* **2014**, *7*, 4588−4600.
(28) Qian, J.; Henderson, W. A.; Xu, W.; Bhattacharya, P.; Engelhard, M.; Borodin, O.; Zhang, J.-G. High rate and stable cycling of lithium metal anode. *Nat. Commun.* **2015**, *6* (1), 6362.
(29) Xu, Z.; Wang, J.; Yang, J.; Miao, X.; Chen, R.; Qian, J.; Miao, R. Enhanced Performance of a Lithium-Sulfur Battery Using a Carbonate-Based Electrolyte. *Angew. Chem., Int. Ed.* **2016**, *55* (35), 10372−10375.
(30) Fanous, J.; Wegner, M.; Grimminger, J.; Andresen, A.; Buchmeiser, M. R. Structure-Related Electrochemistry of Sulfur-Poly(acrylonitrile) Composite Cathode Materials for Rechargeable Lithium Batteries. *Chem. Mater.* **2011**, *23* (22), 5024−5028.
(31) Mikhaylik, Y. V. Electrolytes for lithium sulfur cells. U.S. Patent 7,352,680, 2008.
(32) Li, W.; Yao, H.; Yan, K.; Zheng, G.; Liang, Z.; Chiang, Y.-M.; Cui, Y. The synergetic effect of lithium polysulfide and lithium nitrate to prevent lithium dendrite growth. *Nat. Commun.* **2015**, *6* (1), 7436.
(33) Shin, E. S.; Kim, K.; Oh, S. H.; Cho, W. I. Polysulfide dissolution control: the common ion effect. *Chem. Commun.* **2013**, *49* (20), 2004−2006.
(34) Zhang, Y. Z.; Liu, S.; Li, G. C.; Li, G. R.; Gao, X. P. Sulfur/polyacrylonitrile/carbon multi-composites as cathode materials for lithium/sulfur battery in the concentrated electrolyte. *J. Mater. Chem. A* **2014**, *2* (13), 4652−4659.
(35) Qu, C.; Chen, Y.; Yang, X.; Zhang, H.; Li, X.; Zhang, H. LiNO3-free electrolyte for Li-S battery: A solvent of choice with low Ksp of polysulfide and low dendrite of lithium. *Nano Energy* **2017**, *39*, 262−272.
(36) Zhou, J.; Guo, Y.; Liang, C.; Cao, L.; Pan, H.; Yang, J.; Wang, J. A new ether-based electrolyte for lithium sulfur batteries using a S@pPAN cathode. *Chem. Commun.* **2018**, *54* (43), 5478−5481.
(37) Chen, S.; Zheng, J.; Yu, L.; Ren, X.; Engelhard, M. H.; Niu, C.; Lee, H.; Xu, W.; Xiao, J.; Liu, J.; Zhang, J.-G. High-Efficiency Lithium Metal Batteries with Fire-Retardant Electrolytes. *Joule* **2018**, *2* (8), 1548−1558.
(38) Yang, H.; Guo, C.; Chen, J.; Naveed, A.; Yang, J.; Nuli, Y.; Wang, J. An Intrinsic Flame-Retardant Organic Electrolyte for Safe Lithium-Sulfur Batteries. *Angew. Chem., Int. Ed.* **2019**, *58* (3), 791−795.
(39) Liu, H.; Holoubek, J.; Zhou, H.; Chen, A.; Chang, N.; Wu, Z.; Yu, S.; Yan, Q.; Xing, X.; Li, Y.; et al. Ultrahigh coulombic efficiency electrolyte enables Li||SPAN batteries with superior cycling performance. *Mater. Today* **2021**, *42*, 17−28.
(40) Wu, Z.; Liu, H.; Holoubek, J.; Anderson, C.; Shi, L.; Khemchandani, H.; Lu, D.; Liu, D.; Niu, C.; Xiao, J.; Liu, P. The Role of Ion Transport in the Failure of High Areal Capacity Li Metal Batteries. *ACS Energy Lett.* **2022**, *7* (8), 2701−2710.
(41) Bai, P.; Li, J.; Brushett, F. R.; Bazant, M. Z. Transition of lithium growth mechanisms in liquid electrolytes. *Energy Environ. Sci.* **2016**, *9* (10), 3221−3229.
(42) He, X.; Ren, J.; Wang, L.; Pu, W.; Jiang, C.; Wan, C. Expansion and shrinkage of the sulfur composite electrode in rechargeable lithium batteries. *J. Power Sources* **2009**, *190* (1), 154−156.
(43) Zhang, X.; Gao, P.; Wu, Z.; Engelhard, M. H.; Cao, X.; Jia, H.; Xu, Y.; Liu, H.; Wang, C.; Liu, J.; et al. Pinned Electrode/Electrolyte Interphase and Its Formation Origin for Sulfurized Polyacrylonitrile Cathode in Stable Lithium Batteries. *ACS Appl. Mater. Interfaces* **2022**, *14* (46), 52046−52057.
(44) Xing, X.; Li, Y.; Wang, X.; Petrova, V.; Liu, H.; Liu, P. Cathode electrolyte interface enabling stable Li-S batteries. *Energy Storage Mater.* **2019**, *21*, 474−480.
(45) Shen, Z.; Zhang, W.; Mao, S.; Li, S.; Wang, X.; Lu, Y. Tailored Electrolytes Enabling Practical Lithium-Sulfur Full Batteries via Interfacial Protection. *ACS Energy Lett.* **2021**, *6* (8), 2673−2681.
(46) Holoubek, J.; Liu, H.; Wu, Z.; Yin, Y.; Xing, X.; Cai, G.; Yu, S.; Zhou, H.; Pascal, T. A.; Chen, Z.; Liu, P. Tailoring electrolyte solvation for Li metal batteries cycled at ultra-low temperature. *Nat. Energy* **2021**, *6* (3), 303−313.
(47) Ma, T.; Ni, Y.; Wang, Q.; Zhang, W.; Jin, S.; Zheng, S.; Yang, X.; Hou, Y.; Tao, Z.; Chen, J. Optimize Lithium Deposition at Low Temperature by Weakly Solvating Power Solvent. *Angew. Chem., Int. Ed.* **2022**, *61* (39), No. e202207927.
(48) Kong, X.; Kong, Y.; Liao, X.; Liu, S.; Zhao, Y. A novel mixed ether-based electrolyte for lithium-sulfur batteries with Li anode protection by dual salts. *Sustainable Energy Fuels* **2022**, *6* (15), 3658−3668.
(49) Li, S.; Jiang, M.; Xie, Y.; Xu, H.; Jia, J.; Li, J. Developing High-Performance Lithium Metal Anode in Liquid Electrolytes: Challenges and Progress. *Adv. Mater.* **2018**, *30* (17), 1706375.
(50) Ren, X.; Chen, S.; Lee, H.; Mei, D.; Engelhard, M. H.; Burton, S. D.; Zhao, W.; Zheng, J.; Li, Q.; Ding, M. S.; et al. Localized High-Concentration Sulfone Electrolytes for High-Efficiency Lithium-Metal Batteries. *Chem* **2018**, *4* (8), 1877−1892.
(51) Liu, G.; Cao, Z.; Wang, P.; Ma, Z.; Zou, Y.; Sun, Q.; Cheng, H.; Cavallo, L.; Li, S.; Li, Q.; Ming, J. A.-O. Switching Electrolyte Interfacial Model to Engineer Solid Electrolyte Interface for Fast Charging and Wide-Temperature Lithium-Ion Batteries. *Adv. Sci.* **2022**, *9* (26), 01893.
(52) Ren, X.; Zou, L.; Cao, X.; Engelhard, M. H.; Liu, W.; Burton, S. D.; Lee, H.; Niu, C.; Matthews, B. E.; Zhu, Z.; et al. Enabling High-Voltage Lithium-Metal Batteries under Practical Conditions. *Joule* **2019**, *3* (7), 1662−1676.
(53) Aroca, R.; Nazri, M.; Nazri, G. A.; Camargo, A. J.; Trsic, M. Vibrational Spectra and Ion-Pair Properties of Lithium Hexafluorophosphate in Ethylene Carbonate Based Mixed-Solvent Systems for Lithium Batteries. *J. Solution Chem.* **2000**, *29* (10), 1047−1060.
(54) Seo, D. M.; Boyle, P. D.; Sommer, R. D.; Daubert, J. S.; Borodin, O.; Henderson, W. A. Solvate Structures and Spectroscopic Characterization of LiTFSI Electrolytes. *J. Phys. Chem. B* **2014**, *118* (47), 13601−13608.
(55) Hou, T.; Fong, K. D.; Wang, J.; Persson, K. A. The solvation structure, transport properties and reduction behavior of carbonate-

https://doi.org/10.1021/acsenergylett.3c01711
ACS Energy Lett. 2023, 8, 4818−4830

based electrolytes of lithium-ion batteries. *Chemical Science* **2021**, *12* (44), 14740−14751.
(56) Chen, X.; Hou, T.-Z.; Li, B.; Yan, C.; Zhu, L.; Guan, C.; Cheng, X.-B.; Peng, H.-J.; Huang, J.-Q.; Zhang, Q. Towards stable lithium-sulfur batteries: Mechanistic insights into electrolyte decomposition on lithium metal anode. *Energy Storage Mater.* **2017**, *8*, 194−201.
(57) Chen, Y.; Yu, Z.; Rudnicki, P.; Gong, H.; Huang, Z.; Kim, S. C.; Lai, J.-C.; Kong, X.; Qin, J.; Cui, Y.; Bao, Z. Steric Effect Tuned Ion Solvation Enabling Stable Cycling of High-Voltage Lithium Metal Battery. *J. Am. Chem. Soc.* **2021**, *143* (44), 18703−18713.
(58) Holoubek, J.; Kim, K.; Yin, Y.; Wu, Z.; Liu, H.; Li, M.; Chen, A.; Gao, H.; Cai, G.; Pascal, T. A.; et al. Electrolyte design implications of ion-pairing in low-temperature Li metal batteries. *Energy Environ. Sci.* **2022**, *15* (4), 1647−1658.
(59) Zhang, P.; Jin, H.; Wang, T.; Wang, M. Insight into the effect of lithium-dendrite suppression by lithium bis(fluorosulfony)imide/1,2-dimethoxyethane electrolytes. *Electrochim. Acta* **2018**, *277*, 116−126.
(60) Xu, K. *Electrolytes, Interfaces and Interphases: Fundamentals and Applications in Batteries*; Royal Society of Chemistry, 2023.
(61) Liang, J.-L.; Sun, S.-Y.; Yao, N.; Zheng, Z.; Zhang, Q.-K.; Li, B.-Q.; Zhang, X.-Q.; Huang, J.-Q. Regulating the electrolyte solvation structure by weakening the solvating power of solvents for stable lithium metal batteries. *Sci. China Chem.* **2023**, DOI: 10.1007/s11426-023-1730-x.
(62) Henry, J. S. S. On the Concentration at the Electrodes in a Solution, with special reference to the Liberation of Hydrogen by Electrolysis of a Mixture of Copper Sulphate and Sulphuric Acid. *Proc. Phys. Soc. London* **1899**, *17* (1), 496.
(63) Kim, S. C.; Wang, J.; Xu, R.; Zhang, P.; Chen, Y.; Huang, Z.; Yang, Y.; Yu, Z.; Oyakhire, S. T.; Zhang, W. High-entropy electrolytes for practical lithium metal batteries. *Nat. Energy* **2023**, *8*, 814.

https://doi.org/10.1021/acsenergylett.3c01711
ACS Energy Lett. 2023, 8, 4818−4830